

CombAlign: Enhancing Model Expressiveness in Unsupervised Graph Alignment

Songyang Chen, Yu Liu, Lei Zou, Zexuan Wang, Youfang Lin

Abstract—Unsupervised graph alignment finds the node correspondence between a pair of attributed graphs by only exploiting graph structure and node features. One category of recent studies first computes the node representation and then matches nodes with the largest embedding-based similarity, while the other category reduces the problem to optimal transport (OT) via Gromov-Wasserstein learning. However, it remains largely unexplored in the model expressiveness, as well as how theoretical expressivity impacts prediction accuracy. We investigate the model expressiveness from two aspects. First, we characterize the model’s *discriminative power* in distinguishing matched and unmatched node pairs across two graphs. Second, we study the model’s capability of guaranteeing *node matching properties* such as one-to-one matching and mutual alignment. Motivated by our theoretical analysis, we put forward a hybrid approach named CombAlign with stronger expressive power. Specifically, we enable cross-dimensional feature interaction for OT-based learning and propose an embedding-based method inspired by the Weisfeiler-Lehman test. We also apply non-uniform marginals obtained from the embedding-based modules to OT as priors for more expressiveness. Based on that, we propose a traditional algorithm-based refinement, which combines our OT and embedding-based predictions using the ensemble learning strategy and reduces the problem to maximum weight matching. With carefully designed edge weights, we ensure those matching properties and further enhance prediction accuracy. By extensive experiments, we demonstrate a significant improvement of 14.5% in alignment accuracy compared to state-of-the-art approaches and confirm the soundness of our theoretical analysis.

Index Terms—Unsupervised graph alignment, Model expressiveness, Gromov-Wasserstein discrepancy, Graph learning

I. INTRODUCTION

THE unsupervised graph alignment problem predicts the node correspondence between two attributed graphs, given their topological structure and node features as inputs. It has a wide range of applications such as linking the same identity across different social networks [1], [2], [3], matching scholar accounts between multiple academic platforms [4], [5], and various computer vision tasks [6], [7]. Since the nodes to be aligned do not necessarily have identical graph structure and node features, the problem is challenging, especially in the *unsupervised* setting without any known node correspondence.

Significant research efforts have been dedicated to the unsupervised graph alignment problem. Early work [8], [9],

[10], [11], [12], [13] often formulates the task as the maximum common subgraph isomorphism or the quadratic assignment problem, of which the complexities are NP-hard. In recent years, learning-based methods [14], [15], [16], [17], [3], [18] have garnered increasing attention, surpassing traditional solutions in terms of alignment accuracy. One prominent category of them [14], [15], [16] relies on the “*embed-then-cross-compare*” paradigm. These methods first learn the embedding of each node in both graphs by exploiting the graph structure and node feature information, for example, with graph neural networks (GNNs). Then, two nodes are matched if their embeddings are close according to some specific metric such as cosine similarity [16]. However, for the unsupervised scenario, it is non-trivial to design an optimization objective that is fully suitable for the graph alignment task without any known node correspondence, which poses challenges for learning high-quality embeddings. The most recent work [16] employs a parameter-free approach without an explicit objective to achieve state-of-the-art performance. Another recent line of research [17], [3], [19], [18] generally models the graph alignment problem via *optimal transport* (OT) and achieves promising accuracy due to its well-defined objective. Given the marginal distributions on two finite sets and a predefined transformation cost between them, the OT problem finds the joint distribution to minimize the total transport cost [20]. It has been shown that unsupervised graph alignment can be reduced to OT with the help of Gromov-Wasserstein discrepancy (GWD) [17], [3], [21], which shares similar ideas with node alignment [3], [17]. For approaches of this paradigm, the crux lies in the definition of pair-wise cost within each graph (i.e., *intra-graph* cost), then the transport cost (i.e., *inter-graph* cost) is computed accordingly. We have witnessed an increasingly sophisticated design of intra-graph cost [17], [3], [18] for better matching accuracy.

Unfortunately, it remains largely unexplored for the *theoretical capability* of deep learning-based solutions. We first investigate the model expressiveness for unsupervised graph alignment in the ability to distinguish matched and unmatched node pairs. As shown in Figure 1(a) where u_i is assumed to align to v_i for $i \in \{1, \dots, 5\}$, we see both embedding and optimal transport-based methods as learning a (parameterized) function f that maps two nodes in different graphs to some metric space. For the implementation of f , embedding-based approaches usually compute the similarity between node pairs from the node representation obtained by graph neural networks (GNNs), while optimal transport-based approaches predict the pair-wise alignment probability according to the transport cost between them. To this end, the model accuracy

Songyang Chen, Yu Liu, Zexuan Wang, and Youfang Lin are with the School of Computer and Information Technology, Beijing Jiaotong University, Beijing 100044, China, and the Beijing Key Laboratory of Traffic Data Analysis and Mining, Beijing 100044, China. Lei Zou is with Peking University, Beijing 100871, China. Yu Liu is the corresponding author. E-mail: songyangchen@bjtu.edu.cn; yul@bjtu.edu.cn; zoulei@pku.edu.cn; zexuanwang@bjtu.edu.cn; yflin@bjtu.edu.cn.

Manuscript received xx xx, xxxx; revised xx xx, xxxx.

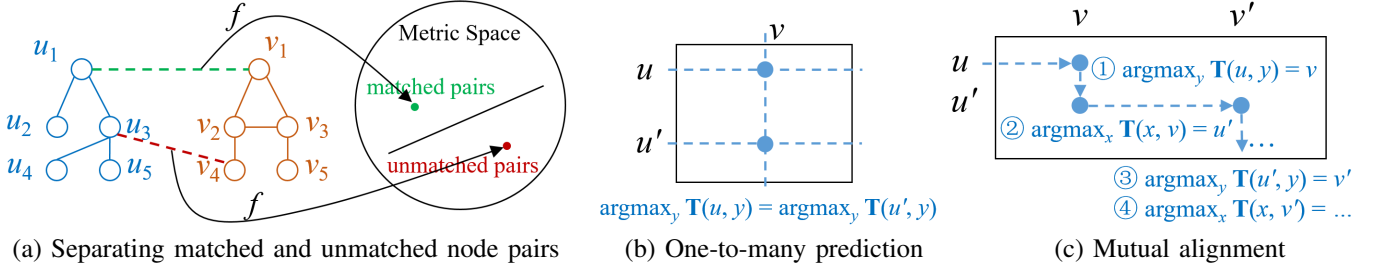


Fig. 1. Illustration of model expressiveness for graph alignment, where (a) denotes the model’s capability of separating matched and unmatched node pairs, while (b) & (c) showcase two disadvantages of pure learning-based approaches, i.e., one-to-many prediction regardless of the one-to-one matching constraint, and the inconsistency between row and column-wise alignment.

is suggested to be closely related to the discriminative power of the specific design of f .

Next, we regret to find that two major disadvantages exist for pure learning-based approaches, which violate the property of graph alignment and deteriorate accuracy. On the one hand, we note that the *one-to-one* matching constraint is forced in scenarios such as the alignment of the protein-protein interaction networks [22] because the conservative functional modules must be uniquely mapped. Although being the *de facto* setting for most studies [15], [18], [3], [16], [17], [23], [24], [25], [26], [27], [28], these methods typically produce one-to-many predictions (Figure 1(b)) since they compute a matrix of matching probability for every pair of nodes and then take the row/column-wise maximum as the prediction. On the other hand, as aligned nodes are paired up in nature, the alignment is *mutual* (i.e., bidirectional). However, predicting the alignment directly via a probability-based approach might lead to inconsistency. As shown in Figure 1(c), for node u , its matched node (i.e., v) should be aligned to another node u' according to the alignment probabilities. We tackle these disadvantages of pure learning-based approaches to enhance model’s theoretical soundness and prediction accuracy.

Motivated by our viewpoint of model expressiveness, we improve the graph alignment process from the following aspects. First, we enhance the optimal transport-based paradigm [3], [18], [17], which has a well-defined objective, by incorporating *feature transformation* along with the well-adopted feature propagation [3], [18] in the transport cost design of GW learning. We prove that more discriminative power is obtained by enabling the cross-dimension mixture of features, which helps to distinguish matched and unmatched node pairs. As we demonstrate in Section IV, with this single optimization, our model outperforms existing OT and embedding-based state of the art. Second, instead of proposing complicated heuristics (e.g., [16]) under the embedding-based framework, we opt for a simple yet effective approach by using parameter-free GNNs to simulate the Weisfeiler-Lehman (WL) algorithm [29]. We also exploit embedding-based prior knowledge to improve the well-formed OT objective, more specifically, we compute *non-uniform marginals* for OT, a vital input to the learning process. The learning algorithm is proved to be more expressive by optimizing an orthogonal aspect to feature transformation. Third, to solve the disadvantages in Figure 1(b) & (c), we reduce graph alignment to the *maximum*

weight matching problem [30], [31] by properly establishing a set of weighted edges between two node sets. To define the edge weights, which determine the matching accuracy, we combine the predictions of our OT and embedding-based procedures via an ensemble learning strategy [32], [33] named *stacking*. Our model not only guarantees the matching properties but also improves prediction accuracy by combining the best of both worlds. We present a model framework named CombAlign to unify the aforementioned modules in a principled way.

Our contributions for the unsupervised graph alignment problem are summarized as follows:

- We combine optimal transport and embedding-based approaches to improve the model expressiveness in *distinguishing matched and unmatched node pairs*. In particular, we demonstrate the necessity of feature transformation and non-uniform marginals in the learning process.
- We transform unsupervised graph alignment into a maximum-weight matching problem with an ensemble learning strategy to integrate embedding and OT-based predictions. This not only ensures important matching properties but also enhances prediction accuracy.
- We propose CombAlign, a unified framework for unsupervised graph alignment to fully integrate the advantages of embedding-based, OT-based, and traditional algorithm-based solutions.
- Extensive experiments are conducted to evaluate our algorithm against both embedding and OT-based state of the art. Our method improves alignment accuracy by a significant margin within less time, while a detailed evaluation shows the effectiveness of each proposed module.

II. PRELIMINARY

Problem Statement. We denote an undirected and attributed graph as $\mathcal{G} = (\mathcal{V}, \mathcal{E}, \mathbf{X})$ with node set \mathcal{V} of size n , edge set \mathcal{E} represented by the adjacency matrix $\mathbf{A} \in \{0, 1\}^{n \times n}$, and $\mathbf{X} \in \mathbb{R}^{n \times d}$ corresponds to the node feature matrix with d -dimensional attribute vectors. We list frequently used notations in Table I.

Definition 1 (Unsupervised Graph Alignment). *Given source graph \mathcal{G}_s and target graph \mathcal{G}_t , without any known anchor node pairs, unsupervised graph alignment returns a set of matched node pairs \mathcal{M} . For each node pair $(u_i, v_k) \in \mathcal{M}$, we have $u_i \in \mathcal{G}_s$ and $v_k \in \mathcal{G}_t$.*

We assume that $n_1 = |\mathcal{V}_s|$, $n_2 = |\mathcal{V}_t|$, and $n_1 \leq n_2$ w.l.o.g. In particular, we focus on the setting of *one-to-one* node alignment, following most existing studies [25], [23], [15], [14], [16], [17], [3], [18]. That is, every node can appear at most once in \mathcal{M} . Instead of directly computing \mathcal{M} , existing learning-based approaches [15], [14], [16], [17], [3], [18] predict an *alignment probability matrix* \mathbf{T} of size $n_1 \times n_2$, where $\mathbf{T}(i, k)$ denotes the probability that $u_i \in \mathcal{G}_s$ is matched to $v_k \in \mathcal{G}_t$. Next, it is sufficient to set $\mathcal{M}(u_i) = \arg \max_k \mathbf{T}(i, k)$. Similar to existing works [3], [18], [14], [15], [16], this work primarily focuses on attributed graphs.

Gromov-Wasserstein (GW) Learning. The discrete form of the Gromov-Wasserstein discrepancy is defined as follows.

Definition 2 (Gromov-Wasserstein Discrepancy (GWD) [17]). *Given the distribution μ (resp. ν) over \mathcal{V}_s (resp. \mathcal{V}_t), the GW discrepancy between μ and ν is defined as*

$$\min_{\mathbf{T} \in \Pi(\mu, \nu)} \sum_{i=1}^{n_1} \sum_{j=1}^{n_1} \sum_{k=1}^{n_2} \sum_{l=1}^{n_2} |\mathbf{C}_s(i, j) - \mathbf{C}_t(k, l)|^2 \mathbf{T}(i, k) \mathbf{T}(j, l), \quad (1)$$

$$\text{s.t. } \mathbf{T} \mathbf{1}_{n_2} = \mu, \mathbf{T}^\top \mathbf{1}_{n_1} = \nu.$$

Here, $\mathbf{C}_s \in \mathbb{R}^{n_1 \times n_1}$ and $\mathbf{C}_t \in \mathbb{R}^{n_2 \times n_2}$ are the *intra-graph costs* for \mathcal{G}_s and \mathcal{G}_t , respectively, which measure the similarity (or distance) of two nodes within each graph [21]. We have $\sum_{i=1}^{n_1} \sum_{k=1}^{n_2} \mathbf{T}(i, k) = 1$ according to the constraints in Equation 1, i.e., \mathbf{T} is the joint probability distribution over two node sets, and $\mathbf{1}_n$ denotes the all-ones vector in \mathbb{R}^n . Let $\mathbf{C}_{gwd} \in \mathbb{R}^{n_1 \times n_2}$ be the *inter-graph cost matrix* [17], [21]:

$$\mathbf{C}_{gwd}(i, k) = \sum_{j=1}^{n_1} \sum_{l=1}^{n_2} |\mathbf{C}_s(i, j) - \mathbf{C}_t(k, l)|^2 \mathbf{T}(j, l). \quad (2)$$

The above definition of \mathbf{C}_{gwd} can be interpreted as follows. Noticing that Equation 1 can be reformulated as

$$\langle \mathbf{C}_{gwd}, \mathbf{T} \rangle = \sum_{i=1}^{n_1} \sum_{k=1}^{n_2} \mathbf{C}_{gwd}(i, k) \mathbf{T}(i, k). \quad (3)$$

To minimize this objective with the constraints of \mathbf{T} , a negative correlation between the values of $\mathbf{C}_{gwd}(i, k)$ and $\mathbf{T}(i, k)$ is encouraged [20]. More precisely, for likely matched node pairs (u_i, v_k) and (u_j, v_l) , $|\mathbf{C}_s(i, j) - \mathbf{C}_t(k, l)|^2$ should be small, i.e., the values of $\mathbf{C}_s(i, j)$ and $\mathbf{C}_t(k, l)$ are close [17], [3].

The Optimal Transport (OT) Problem. Actually, Equation 3 can be interpreted via optimal transport. Given $\mathbf{C} \in \mathbb{R}^{n_1 \times n_2}$ which represents the cost of transforming probability distribution μ to ν , we compute the joint probability distribution $\mathbf{T} \in \mathbb{R}^{n_1 \times n_2}$ so that the total transport cost is minimized. It can be solved by the Sinkhorn algorithm [34], [35] via an iterative procedure. With learnable costs, existing solutions [17], [3], [18] adopt the proximal point method [36] to reduce GW learning to OT and to learn the alignment probability and parameters in the cost term jointly.

Graph Neural Network (GNN). To integrate the local graph structures and node features for node representation learning, one prominent approach is the graph neural networks [37], [38], [39], which generally contains two steps, namely, *feature propagation* (i.e., message passing) across neighbors and *feature transformation* with a learnable transformation matrix.

TABLE I
TABLE OF NOTATIONS.

Notation	Description
$\mathcal{G}_s, \mathcal{G}_t$	The source and target graphs
$\mathbf{A}_p, \mathbf{X}_p$	Adjacency matrix, node feature matrix ($p = s, t$)
u_i, u_j, v_k, v_l	Nodes with $u_i, u_j \in \mathcal{G}_s$ and $v_k, v_l \in \mathcal{G}_t$
$\mathbf{Z}_p, \mathbf{H}_p, \mathbf{R}_p$	Embeddings computed by GNN, GNN w/o training, and feature propagation, respectively ($p = s, t$)
$\mathbf{C}_s, \mathbf{C}_t, \mathbf{C}_{gwd}$	Intra-graph and inter-graph costs for GW learning
$\mathbf{T}_{WL}, \mathbf{T}_{GW}$	The alignment probability matrices
$f(\cdot), g(\cdot)$	Functions with and without learnable parameters

III. OUR PROPOSED MODEL

A. Model Overview

We present an overview of our CombAlign model, which incorporates embedding-based, OT-based, and traditional techniques to tackle unsupervised graph alignment with theoretical improvements. The framework is shown in Figure 2.

As illustrated in Algorithm 1, given graphs \mathcal{G}_s and \mathcal{G}_t , CombAlign first predicts the alignment probabilities by employing two separate approaches. Specifically, the *WL-then-Inner-Product* (WL) module obtains the embedding-based alignment probability \mathbf{T}_{WL} by simulating the Weisfeiler-Leman (WL) algorithm [29] (Line 1). Based on that, the *Non-Uniform Marginal* (NUM) module computes two marginal distributions on node sets, which serve as inputs to the next step (Line 2). The following *Unsupervised GW Learning with Feature Transformation* (GRAFT) module derives an OT-based prediction \mathbf{T}_{GW} with enhanced model expressivity (Line 3). Finally, the *Combine* module integrates both alignment matrices \mathbf{T}_{WL} and \mathbf{T}_{GW} , and employs a traditional algorithm-based solution to further improve matching accuracy (Lines 4-5), as well as to guarantee alignment properties (Cf. Figure 1).

Algorithm 1: The CombAlign Algorithm

Input: Attributed graphs $\mathcal{G}_s(\mathbf{A}_s, \mathbf{X}_s)$ and $\mathcal{G}_t(\mathbf{A}_t, \mathbf{X}_t)$
Output: The set of predicted node matching \mathcal{M}

- 1 $\mathbf{T}_{WL} \leftarrow \text{WL}(\mathcal{G}_s, \mathcal{G}_t)$; // Algorithm 4
- 2 $\mu, \nu \leftarrow \text{NUM}(\mathbf{T}_{WL})$; // Algorithm 5
- 3 $\mathbf{T}_{GW} \leftarrow \text{GRAFT}(\mathcal{G}_s, \mathcal{G}_t, \mu, \nu)$; // Algorithm 3
- 4 $\mathcal{M} \leftarrow \text{Combine}(\mathbf{T}_{WL}, \mathbf{T}_{GW})$; // Algorithm 6
- 5 **return** \mathcal{M} ;

B. Improving Model's Discriminative Power

We elaborate on the designed modules by focusing on their discriminative power for graph alignment. We first introduce the GRAFT module followed by the WL and NUM modules as the latter two further enhance the expressiveness of the former.

1) *The GW Learning (GRAFT) Module:* It comprises embedding-based feature propagation and transformation followed by the GW learning step with the idea of OT.

Feature Propagation and Transformation. As pointed out by [3], for OT-based approaches, the alignment quality heavily depends on the specific design of intra-graph costs \mathbf{C}_s and

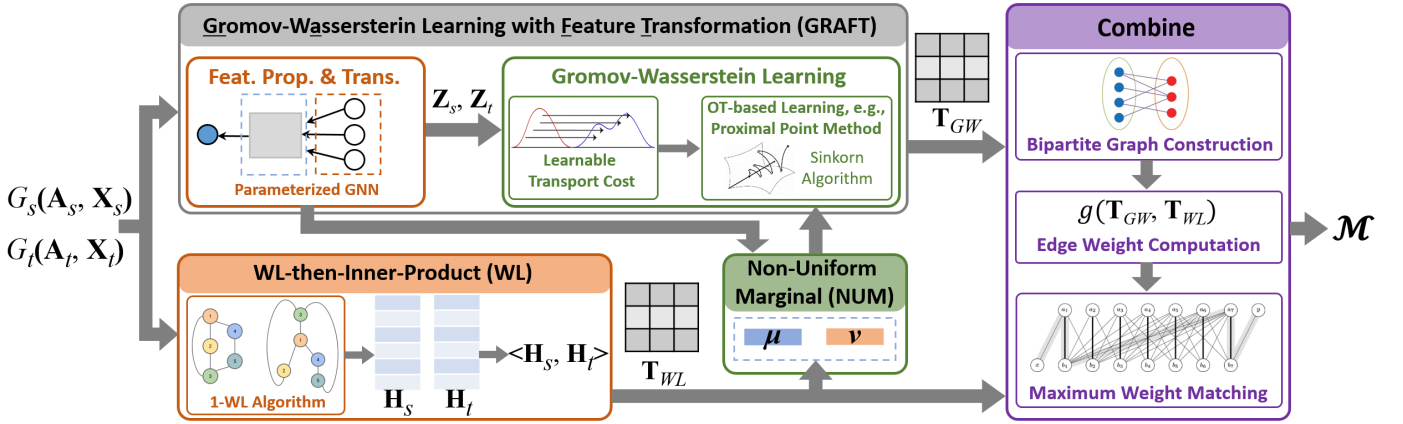


Fig. 2. The overall framework of CombAlign. Modules in orange, green, and purple belong to the embedding-based, OT-based, and traditional algorithm-based approaches, respectively.

C_t . Representative methods [17], [3], [18] integrate graph structures and node features as the following equation:

$$\mathbf{R}_p = g_{prop}(\mathbf{A}_p)\mathbf{X}_p, p = s, t, \quad (4)$$

where $g_{prop}(\cdot)$ is a general function without learnable parameters. For example, we can set it to the standard propagation of GCN [40], i.e., $g_{prop}(\mathbf{A}) = \tilde{\mathbf{D}}^{-\frac{1}{2}}\tilde{\mathbf{A}}\tilde{\mathbf{D}}^{-\frac{1}{2}}$ with $\tilde{\mathbf{D}} = \tilde{\mathbf{A}}\mathbf{1}$ and $\tilde{\mathbf{A}} = \mathbf{A} + \mathbf{I}$. We use $\mathbf{R}_s \in \mathbb{R}^{n_1 \times d}$ and $\mathbf{R}_t \in \mathbb{R}^{n_2 \times d}$ to denote the result embedding matrices and refer to the process as *feature propagation*¹.

We observe that this step only enables the propagation of features between a node and its neighbors in a *dimension-by-dimension* manner. However, interaction across different feature dimensions is not considered, which is also important, for example, when two feature dimensions share similar semantics. We put forward feature transformation, which is widely adopted by classical GNNs [40], [41], [42] and is formulated as

$$\mathbf{Z}_p = f_{GNN}(\mathbf{A}_p, \mathbf{X}_p, \mathbf{W}), p = s, t. \quad (5)$$

Here, f_{GNN} is a learnable function, and \mathbf{W} denotes the learnable transformation matrices and is shared by two graphs, which enables feature interaction *across dimensions*. The following theorem demonstrates that, within the GW learning framework, the adoption of a single transformation layer for feature interaction enhances the discriminative power of the intra-graph cost matrices.

Theorem III.1. *We are given the graph structures $\mathbf{A}_s, \mathbf{A}_t$ and node features $\mathbf{X}_s, \mathbf{X}_t$ as input. Denote feature propagation as $\mathbf{R}_p = g(\mathbf{A}_p)\mathbf{X}_p, p = s, t$, where $g(\cdot)$ is a function without learnable parameters. Denote the additional linear transformation as $\mathbf{Z}_p = \mathbf{R}_p\mathbf{W}$, where $\mathbf{W} \in \mathbb{R}^{d \times d}$ is the learnable matrix. Assume that we set the intra-graph cost matrices as $\mathbf{C}'_p = \mathbf{R}_p\mathbf{R}_p^\top$ and $\mathbf{C}_p = \mathbf{Z}_p\mathbf{Z}_p^\top$ for $p = s, t$, respectively, and let $(u_i, v_k), (u_j, v_l) \in \mathcal{M}^*$ and $(u_{j'}, v_l) \notin \mathcal{M}^*$ where \mathcal{M}^* is the ground truth. Then, there exists a*

case that $|\mathbf{C}'_s(i, j) - \mathbf{C}'_t(k, l)| = |\mathbf{C}'_s(i, j') - \mathbf{C}'_t(k, l)|$ and $|\mathbf{C}_s(i, j) - \mathbf{C}_t(k, l)| \neq |\mathbf{C}_s(i, j') - \mathbf{C}_t(k, l)|$.

Proof. First note that if an algorithm is able to separate $|\mathbf{C}_s(i, j) - \mathbf{C}_t(k, l)|$ and $|\mathbf{C}_s(i, j') - \mathbf{C}_t(k, l)|$, or more specifically, to learn that $|\mathbf{C}_s(i, j) - \mathbf{C}_t(k, l)| < |\mathbf{C}_s(i, j') - \mathbf{C}_t(k, l)|$, it is more likely to make the correct prediction $(\mathbf{T}(j, l) > \mathbf{T}(j', l))$. Now assume that \mathbf{X}_s contains different one-hot features for each node, and the distance between u_i and u_j (resp. $u_{j'}$) is beyond twice of K , the maximum step of feature propagation. For simplicity, let i, j , and j' be the corresponding index. Since u_i cannot propagate any information to u_j and $u_{j'}$ (and vice versa), we have $\mathbf{R}_s(u_i, j) = 0, \mathbf{R}_s(u_i, j') = 0, \mathbf{R}_s(u_j, i) = 0$, and $\mathbf{R}_s(u_{j'}, i) = 0$. Thus, we have $\mathbf{R}_s(u_i)^\top \mathbf{R}_s(u_j) = \mathbf{R}_s(u_i)^\top \mathbf{R}_s(u_{j'}) = 0$, i.e., $\mathbf{C}'_s(i, j) = \mathbf{C}'_s(i, j') = 0$.

With the linear transformation matrix \mathbf{W} , different dimensions of the one-hot features are directly interacted. We might have $\mathbf{Z}_s(u_i)^\top \mathbf{Z}_s(u_j) \neq 0$ and $\mathbf{Z}_s(u_i)^\top \mathbf{Z}_s(u_{j'}) = 0$ by setting the corresponding columns of \mathbf{W} . More generally, by learning \mathbf{W} , it is possible to have $\mathbf{Z}_s(u_i)^\top \mathbf{Z}_s(u_j) \neq \mathbf{Z}_s(u_i)^\top \mathbf{Z}_s(u_{j'})$, and the theorem follows. \square

The following corollary can be easily derived.

Corollary III.2. *Assume that the intra-graph cost matrix \mathbf{C}_p is the linear combination of graph structure \mathbf{A}_p , feature information $\mathbf{X}_p\mathbf{X}_p^\top$, and node embedding $\mathbf{Z}_p\mathbf{Z}_p^\top$, i.e.,*

$$\mathbf{C}_p = \beta_p^{(1)}\mathbf{A}_p + \beta_p^{(2)}\mathbf{X}_p\mathbf{X}_p^\top + \beta_p^{(3)}\mathbf{Z}_p\mathbf{Z}_p^\top, p = s, t, \quad (6)$$

where we use β_p to represent learnable coefficients. If feature transformation is applied to compute \mathbf{Z}_p , the costs have more discriminative power in separating the matched and unmatched node pairs.

Proof. For existing work with such cost formation [3], [18], following Theorem III.1, it can be easily proved that feature transformation still provides more discriminative power. Recall the example in the proof of Theorem III.1. In this case, the first two terms are equal to zero, and the corollary holds. \square

¹Note that [3] uses parameter-free GNN to denote this process. In this paper, we propose strict definitions for both terms and formally analyze their differences.

Corollary III.3. *If the f_{GNN} function has more expressive power in distinguishing node embeddings, e.g. [42], the intra-graph cost has more discriminative power in separating matched and unmatched pairs.*

Proof. For two graphs with $\max(n_1, n_2) = O(n)$, note that we intend to simultaneously hold up to $O(n^2)$ constraints (i.e., matched and unmatched pairs) described in Theorem III.1 by learning the GNN parameters. With a more powerful GNN to distinguish the node embeddings \mathbf{Z}_p , the intra-graph cost terms for different node pairs become more separable. \square

Motivated by the theoretical results, we employ three specific GNN models for feature propagation and transformation:

- Lightweight GCN [43] (single linear transformation):

$$\mathbf{Z} = \text{Concat}(\mathbf{X}, \mathbf{P}\mathbf{X}, \dots, \mathbf{P}^K \mathbf{X}) \mathbf{W}, \mathbf{P} = \tilde{\mathbf{D}}^{-\frac{1}{2}} \tilde{\mathbf{A}} \tilde{\mathbf{D}}^{-\frac{1}{2}}. \quad (7)$$

- Graph Convolutional Network (GCN) [40]:

$$\mathbf{Z}^{(k+1)} = \sigma(\mathbf{P}\mathbf{Z}^{(k)} \mathbf{W}^{(k+1)}), k \in [0, K-1]. \quad (8)$$

- Graph Isomorphism Network (GIN) [42]:

$$\mathbf{Z}^{(k+1)} = \text{MLP}^{(k+1)}((1+\varepsilon^{(k+1)})\mathbf{Z}^{(k)} + \mathbf{A}\mathbf{Z}^{(k)}), k \in [0, K-1]. \quad (9)$$

For GCN and GIN, we use the skip connection to combine node embeddings of all layers: $\mathbf{Z}_p = \sum_{k=1}^K \mathbf{Z}_p^{(k)}$, $p = s, t$. The pseudocode is shown in Algorithm 2.

Algorithm 2: Feature Propagation and Transformation (FeatProp&Trans)

Input: \mathbf{A}, \mathbf{X} , model parameter $\{\mathbf{W}^{(1)}, \dots, \mathbf{W}^{(K)}\}$

Output: Node representation \mathbf{Z}

```

1  $\mathbf{Z}^{(0)} \leftarrow \mathbf{X}$ ;
2 for  $k = 1$  to  $K$  do
3    $\mathbf{Z}^{(k)} \leftarrow \sigma(g_{prop}(\mathbf{A}, \mathbf{Z}^{(k-1)}) \cdot \mathbf{W}^{(k)})$ ;
4 return  $\mathbf{Z} \leftarrow \sum_{k=1}^K \mathbf{Z}^{(k)}$ ;
```

Gromov-Wasserstein Learning. Given the cost matrices as input, we follow the well-adopted approach in [17], [3], [18] by employing the proximal point method [36], [17] and reducing the learning problem to optimal transport [34], [35]. Denote by $L(\mathbf{T}, \beta, \mathcal{W})$ the learning objective in Equation 3, where $\beta = (\beta_s, \beta_t)$ is the learnable coefficients to combine multiple terms for the intra-graph cost and \mathcal{W} denotes the parameters in feature transformation. We update \mathbf{T} and $\Theta = \{\beta, \mathcal{W}\}$ by the proximal point method and gradient descent, respectively.

$$\begin{aligned} \Theta^{(i+1)} &= \arg \min \left\{ \nabla_{\Theta} L(\mathbf{T}^{(i)}, \beta^{(i)}, \Theta^{(i)})^T \Theta + \frac{1}{2\tau_{\Theta}} \|\Theta - \Theta^{(i)}\|^2 \right\} \\ \mathbf{T}^{(i+1)} &= \arg \min \left\{ \nabla_{\mathbf{T}} L(\mathbf{T}^{(i)}, \beta^{(i)}, \Theta^{(i)})^T \mathbf{T} + \frac{1}{\tau_T} \text{KL}(\mathbf{T} \|\mathbf{T}^{(i)}) \right\}. \end{aligned} \quad (10)$$

Note that $\text{KL}(\cdot \|\cdot)$ is the Kullback-Leibler divergence, and $\tau_{\Theta} = (\tau_{\beta}, \tau_{\mathcal{W}})$ is the learning rates for updating β and \mathcal{W} , respectively, while τ_T is the regularization coefficient in the Sinkhorn algorithm. It can be proved that with the simplified version of feature transformation, e.g., by adopting the lightweight GCN, the GW learning procedure theoretically guarantees the convergence result as in [17], [3].

Theorem III.4. *Denote by $L(\mathbf{T}, \beta, \mathcal{W})$ the learning objective in Equation 3. Suppose that $0 < \tau_T < \frac{1}{L_f^T}$, $0 < \tau_{\beta} < \frac{1}{L_f^{\beta}}$, and $0 < \tau_{\mathcal{W}} < \frac{1}{L_f^{\mathcal{W}}}$, where L_f^T , L_f^{β} , and $L_f^{\mathcal{W}}$ are the gradient Lipschitz continuous modulus of $L(\mathbf{T}, \beta, \mathcal{W})$ respectively. If the following conditions hold, i.e.,*

$$\mathcal{T} = \{\mathbf{T} \geq 0 : \mathbf{T}\mathbf{1}_{n_2} = \mu, \mathbf{T}^T \mathbf{1}_{n_1} = \nu\}, \quad (11)$$

$$\mathcal{B} = \{(\beta_s, \beta_t) \geq 0 : \sum_{i=1}^3 \beta_p^{(i)} = 1, p = s, t\}, \quad (12)$$

$$\mathcal{W} = \left\{ \sum_{i=1} \mathbf{W}_{ij} = 1, \forall j \in [1, d] \right\}, \quad (13)$$

then the GW learning process converges to a critical point of $\bar{L}(\mathbf{T}, \beta, \mathcal{W})$, with $\bar{L}(\mathbf{T}, \beta, \mathcal{W}) = L(\mathbf{T}, \beta, \mathcal{W}) + \mathbb{I}_T(\mathbf{T}) + \mathbb{I}_B(\beta) + \mathbb{I}_W(\mathcal{W})$, where $\mathbb{I}_C(\cdot)$ denotes the indicator function on the set C .

Proof. Note that by our definition, \mathcal{T} , \mathcal{B} , and \mathcal{W} are bounded sets, and $L(\mathbf{T}, \beta, \mathcal{W})$ is a bi-quadratic function with respect to \mathbf{T} , β , and \mathcal{W} . To guarantee that \mathcal{W} satisfies the above constraint in each iteration, it is sufficient to apply an activation function (e.g., ReLU) followed by column-wise normalization. The proof then generally follows that of Theorem 5 in [3], where we can compute the gradient of L w.r.t. \mathbf{T} , β , and \mathcal{W} to update the parameters with provable convergence. \square

Algorithm 3: Unsupervised Gromov-Wasserstein Learning with Feature Transformation (GRAFT)

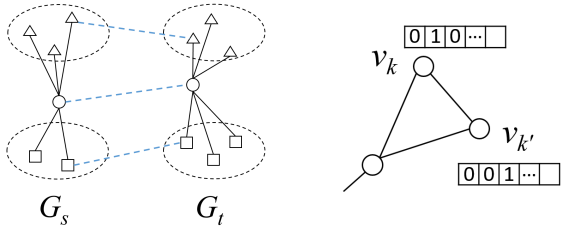
Input: \mathcal{G}_s and \mathcal{G}_t , marginal distributions μ and ν

Output: The OT-based alignment probability \mathbf{T}_{GW}

```

1  $\mathbf{T}_{GW} \leftarrow \mu\nu^T$ ,  $\beta_s, \beta_t \leftarrow (1, 1, 1)^T$ ;
2 for  $i = 1$  to  $I$  do
3    $\mathbf{Z}_s \leftarrow \text{FeatProp\&Trans}(\mathbf{A}_s, \mathbf{X}_s, \mathbf{W}^{(1, \dots, K)})$ ;
4    $\mathbf{Z}_t \leftarrow \text{FeatProp\&Trans}(\mathbf{A}_t, \mathbf{X}_t, \mathbf{W}^{(1, \dots, K)})$ ;
   // intra-graph cost (Eq. 6)
5    $\mathbf{C}_p \leftarrow f_{\beta}(\mathbf{A}_p, \mathbf{X}_p, \mathbf{Z}_p), p = s, t$ ;
   // inter-graph cost (Eq. 1)
6    $\mathbf{C}_{gwd} \leftarrow f_{gwd}(\mathbf{C}_s, \mathbf{C}_t, \mathbf{T}_{GW})$ ;
7   Minimize  $\langle \mathbf{C}_{gwd}, \mathbf{T}_{GW} \rangle$  by updating
    $\Theta = \{\beta, \mathbf{W}^{(1, \dots, K)}\}$ ;
   // the proximal point method
8   Initialize  $\mathbf{T}^{(0)} \leftarrow \mathbf{T}_{GW}$  and  $\mathbf{a} \leftarrow \mu$ ;
9   for  $i' = 0$  to  $I_{ot} - 1$  do
10    Set  $\mathbf{G} \leftarrow \exp\left(-\frac{\mathbf{C}_{gwd}}{\tau_T}\right) \odot \mathbf{T}^{(i')}$ ;
    // Sinkhorn-Knopp algorithm
11    for  $j = 1$  to  $J$  do
12       $\mathbf{b} \leftarrow \frac{\nu}{\mathbf{G}^T \mathbf{a}}$ ;
13       $\mathbf{a} \leftarrow \frac{\mu}{\mathbf{G} \mathbf{b}}$ ;
14     $\mathbf{T}^{(i'+1)} \leftarrow \text{Diag}(\mathbf{a}) \mathbf{G} \text{Diag}(\mathbf{b})$ ;
15   $\mathbf{T}_{GW} \leftarrow \mathbf{T}^{(I_{ot})}$ ;
16 return  $\mathbf{T}_{GW}$ ;
```

The pseudocode of the GRAFT module is demonstrated in Algorithm 3. We first initialize the OT-based alignment matrix \mathbf{T}_{GW} with the input marginals and set the learnable



(a) An illustrative example (b) An inseparable case

Fig. 3. Illustration of the necessity of non-uniform marginals.

coefficients (Line 1). Then, for each iteration (Line 2), we invoke the feature propagation and transformation process to derive node representations (Lines 3-4), based on which the intra and inter-graph costs are computed (Lines 5-6). The GW learning procedure is employed (Lines 7-16), which takes the Sinkhorn algorithm as a subprocedure to iteratively update \mathbf{T}_{GW} , an $n_1 \times n_2$ -sized alignment probability matrix.

2) *The WL-then-Inner-Product (WL) Module:* The WL module uses a GNN with non-learnable parameters (referred to as *parameter-free GNNs*) to simulate the Weisfeiler-Lehman (WL) test [29]. As demonstrated in Algorithm 4, we use K random matrices $\widehat{\mathbf{W}}^{(1)}, \dots, \widehat{\mathbf{W}}^{(K)}$ to resemble the hash functions in WL test (Line 1). Taking node features as input, the algorithm conducts K layers of graph convolution (Lines 2-3), similar to the GNN in Section III-B1 but with non-updated parameters. We denote by \mathbf{H}_s and \mathbf{H}_t the node embeddings in order to distinguish them from those obtained via a learnable GNN (i.e., \mathbf{Z}_s and \mathbf{Z}_t). The embedding-based alignment probability \mathbf{T}_{WL} is obtained by multiplying \mathbf{H}_s and \mathbf{H}_t , followed by the normalization process (Line 4). We first adopt a ReLU activation and then divide each term by the summation of all terms in \mathbf{T}_{WL} . In this way, each element of the returned \mathbf{T}_{WL} denotes the matching probability.

Algorithm 4: WL-then-Inner-Product (WL)

Input: $\mathcal{G}_s(\mathbf{A}_s, \mathbf{X}_s)$ and $\mathcal{G}_t(\mathbf{A}_t, \mathbf{X}_t)$

Output: Embedding-based alignment probability \mathbf{T}_{WL}

- 1 Initialize non-learnable parameters $\widehat{\mathbf{W}}^{(1)}, \dots, \widehat{\mathbf{W}}^{(K)}$;
 - 2 $\mathbf{H}_s \leftarrow \text{FeatProp\&Trans}(\mathbf{A}_s, \mathbf{X}_s, \widehat{\mathbf{W}}^{(1, \dots, K)})$;
 - 3 $\mathbf{H}_t \leftarrow \text{FeatProp\&Trans}(\mathbf{A}_t, \mathbf{X}_t, \widehat{\mathbf{W}}^{(1, \dots, K)})$;
 - 4 $\mathbf{T}_{WL} \leftarrow \text{Norm}(\mathbf{H}_s \mathbf{H}_t^\top)$;
 - 5 **return** \mathbf{T}_{WL} ;
-

Although the prediction of WL is not as precise as GRAFT due to its simplicity, as we will show in the following, it serves as the prior knowledge for the OT-based component to boost matching accuracy.

3) *The Non-Uniform Marginal (NUM) Module:* It improves the GRAFT module by providing non-uniform marginals as prior knowledge. We observe that OT-based approaches take two marginal distributions on \mathcal{V}_s and \mathcal{V}_t as input, which is commonly assumed to be uniformly distributed [17], [3], [18]. However, graphs are typical *non-Euclidean* data where node distributions are not i.i.d. A motivating example is shown in Figure 3(a), where both \mathcal{G}_s and \mathcal{G}_t contain two clusters and a hub node, respectively. Suppose that the correspondence

between nodes is consistent with their shapes. If the pair of hubs is correctly aligned, it might eliminate a large amount of impossible alignments. We formally show that non-uniform marginals indeed enhance the expressive power of GW learning for graph alignment with the following theorem.

Theorem III.5. *Consider the case that $(u_i, v_k) \in \mathcal{M}^*$ and $(u_i, v_{k'}) \notin \mathcal{M}^*$. For GW learning (e.g., GRAFT), under the mild assumption of the intra-graph cost, i.e.,*

$$\mathbf{C}_s(i, i) = a, \forall u_i, \mathbf{C}_t(k, k) = b, \forall v_k, \quad (14)$$

$$\mathbf{C}_s(i, j) = \mathbf{C}_s(j, i), \mathbf{C}_t(k, l) = \mathbf{C}_t(l, k), \forall u_i, u_j, v_k, v_l, \quad (15)$$

$$\mathbf{C}_t(k, l) = \mathbf{C}_t(k', l), \forall v_l \in \mathcal{V}_t \setminus \{v_k, v_{k'}\}, \quad (16)$$

with uniform marginals $\boldsymbol{\mu} = (1/n_1, \dots, 1/n_1)^\top$ and $\boldsymbol{\nu} = (1/n_2, \dots, 1/n_2)^\top$, the first iteration of the GW learning process with $\mathbf{T}^{(0)} = \boldsymbol{\mu}\boldsymbol{\nu}^\top$ cannot determine whether u_i is matched to v_k or $v_{k'}$.

Proof. First, we show that there exists such a case satisfying our assumption. If the embeddings in both \mathbf{X}_p and \mathbf{Z}_p are normalized, we have $\mathbf{X}_p(v)^\top \mathbf{X}_p(v) = \mathbf{Z}_p(v)^\top \mathbf{Z}_p(v) = 1$, thus the first constraint holds. The second constraint is satisfied for undirected graphs if each term of \mathbf{C}_p is computed by the dot product of node embeddings. For the third constraint, an illustrative example is given in Figure 3(b). For two nodes v_k and $v_{k'}$ in \mathcal{G}_t that are automorphism to each other but with different one-hot encodings, after feature propagation, we have $\mathbf{R}_t(v_l, k) = \mathbf{R}_t(v_l, k')$ for each v_l because the propagation strategy is shared by each dimension. Therefore, we have $\mathbf{R}_t(v_l)^\top \mathbf{R}_t(v_k) = \mathbf{R}_t(v_l)^\top \mathbf{R}_t(v_{k'})$, and the constraint follows. This claim also holds with feature transformation if the GNN module cannot separate $\mathbf{Z}_t(v_l)^\top \mathbf{Z}_t(v_k)$ and $\mathbf{Z}_t(v_l)^\top \mathbf{Z}_t(v_{k'})$.

Second, we categorize the terms in $\mathbf{C}_{gwd}(i, k)$ as the following cases (Cf. Equation 2). Note that we have $\mathbf{T}^{(0)}(i, k) = \frac{1}{n_1 n_2}$, $\forall i, k$. Denote by $c_{ik}(j, l)$ the terms in $\mathbf{C}_{gwd}(i, k)$, we have

- $l = k$: $c_{ik}(j, k) = |\mathbf{C}_s(i, j) - \mathbf{C}_t(k, k)|^2 \mathbf{T}(j, k)$,
- $l = k'$: $c_{ik}(j, k') = |\mathbf{C}_s(i, j) - \mathbf{C}_t(k, k')|^2 \mathbf{T}(j, k')$,
- $l \neq k, k'$: $c_{ik}(j, l) = |\mathbf{C}_s(i, j) - \mathbf{C}_t(k, l)|^2 \mathbf{T}(j, l)$.

For each j , by constraint 1 and 2, the summation of the first and second cases are equal for $\mathbf{C}_{gwd}(i, k)$ and $\mathbf{C}_{gwd}(i, k')$. By constraint 3, for each term in the third case, the values are the same for v_k and $v_{k'}$. Then we have $\mathbf{C}_{gwd}(i, k) = \mathbf{C}_{gwd}(i, k')$ in the first iteration of GW learning for each $u_i \in \mathcal{G}_s$, which completes the proof. \square

Note that apart from feature transformation, which improves model's discriminative power via the first part of each term of $\mathbf{C}_{gwd}(i, k)$, i.e., $|\mathbf{C}_s(i, j) - \mathbf{C}_t(k, l)|^2$, we offer another perspective by investigating the second term $\mathbf{T}(j, l)$. To solve this problem, the following heuristics are provided to set non-uniform marginals without extra computational costs.

A fixed prior inspired by WL. We use the prior knowledge obtained from the WL test to set non-uniform marginals $\boldsymbol{\mu}$ and $\boldsymbol{\nu}$. Given the embedding-based alignment probability \mathbf{T}_{WL} , the marginals are computed by row/column-wise summation (shown in Algorithm 5).

Adaptive marginals during GW Learning. Recall that \mathbf{T}_{WL} is obtained by non-learnable embeddings \mathbf{H}_s and \mathbf{H}_t , while

Algorithm 5: Non-Uniform Marginal (NUM)**Input:** Embedding-based alignment probability \mathbf{T}_{WL} **Output:** Two marginal distributions μ, ν

```

1  $\mu \leftarrow \mathbf{T}_{WL} \cdot \mathbf{1}_{n_2}, \nu \leftarrow \mathbf{T}_{WL}^\top \cdot \mathbf{1}_{n_1};$ 
2 return  $\mu, \nu;$ 

```

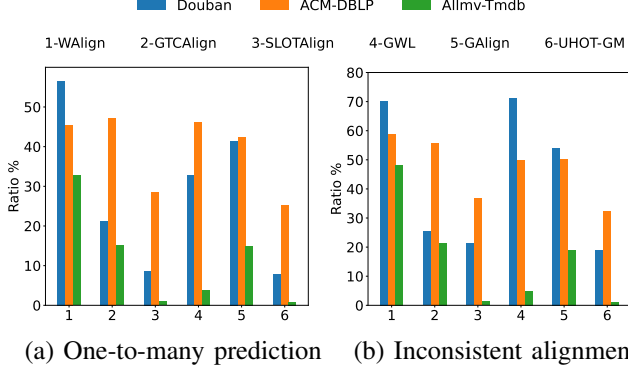


Fig. 4. Percentage of one-to-many predictions and inconsistencies in terms of mutual alignment for representative baselines.

the GRAFT module yields more informative node representation \mathbf{Z}_s and \mathbf{Z}_t through GW learning. Therefore, during each iteration (i.e., Line 2) of Algorithm 3, we use the learnable representations to compute an $n_1 \times n_2$ -sized matrix following Algorithm 4, and take it as the input of Algorithm 5. The marginals are used to initialize the proximal point method (i.e., Lines 8, 12 & 13 of Algorithm 3) and are adjusted on the fly.

C. Ensuring Matching Properties (The Combine Module)

Motivation. As we have pointed out in Figure 1(b) & (c) of Section I, pure learning-based methods [17], [3], [18], [16], [44] fail to guarantee alignment properties such as one-to-one matching and mutual alignment, albeit that they can achieve better practical accuracy than the traditional approaches [8], [9], [10]. In contrast, existing studies (e.g., [22]) have demonstrated real-world scenarios in which one-to-one node matching needs to be ensured. The inconsistency in mutual alignment means that for a predicted matching (u, v) taking from the row/column-wise maximum of the alignment probabilities, we have $\arg \max_y \mathbf{T}(u, y) = v$ and $\arg \max_x \mathbf{T}(x, v) \neq u$. This contradicts the essence of graph alignment where aligned nodes are paired up. We demonstrate in Figure 4 that both problems are prevalent on real-world datasets. Given the output of an algorithm, we calculate the percentages of one-to-many predictions and inconsistencies in terms of mutual alignment, and find that a significant ratio of the predictions violates these alignment properties.

We observe that *maximum weight matching* is a feasible solution to this problem, which has been adopted by traditional approaches. It takes a bipartite graph with weighted edges as input and finds a set of edges with maximum total weight on the condition that selected edges do not share any endpoint (i.e., node). By constructing a bipartite graph from the node sets, finding the maximum weight matching is equivalent to graph alignment with the additional benefit of holding the

matching properties. The remaining challenge is to guarantee the accuracy of the alignment. Intuitively, the edge weights determine the alignment accuracy and should be close to the ground truth alignment. Our solution, referred to as the *Combine* module, tackles this problem by effectively combining both embedding and OT-based alignment probabilities. Specifically, it includes the following steps (Cf. Figure 2).

Bipartite Graph Construction. To construct the bipartite graph \mathcal{G}_b , we set $\mathcal{V}_b = \mathcal{V}_s \cup \mathcal{V}_t$. Instead of building edges for all node pairs, we observe that in most cases, the ground truth is contained in the top- r predictions. As the GRAFT module generally achieves better performance, for each node $u_i \in \mathcal{G}_s$, we connect it to the nodes in \mathcal{G}_t with top- r largest $\mathbf{T}_{GW}(i, \cdot)$. This step reduces the edge number from $n_1 n_2$ to $r n_1$ and significantly improves practical efficiency.

Edge Weight Computation. We adopt the idea of *ensemble learning* (more specifically, *stacking*) and see both embedding and OT-based predictions as base learners. We employ a simple yet effective parameter-free strategy to take the best of both worlds and believe that it tends to obtain more accurate predictions, i.e., the edge weight being close to the ground truth alignment. We consider the following concrete forms of edge weights and use the “both confident” setting by default:

- “Both confident”: $g_{EL}(\mathbf{T}_{WL}, \mathbf{T}_{GW}) = \mathbf{T}_{WL} \odot \mathbf{T}_{GW}$,
- “Simple average”: $g_{EL}(\mathbf{T}_{WL}, \mathbf{T}_{GW}) = (\mathbf{T}_{WL} + \mathbf{T}_{GW})/2$.

Maximum Weight Matching. Note that any maximum weight matching algorithm with real-value weights (e.g., the modified Jonker-Volgenant algorithm (MJV) [45]) can be invoked to solve the problem. The pseudocode of the *Combine* module is shown in Algorithm 6, which returns a set of (one-to-one) matched node pairs instead of the alignment probabilities.

Theorem III.6. *With the Combine module, our algorithm predicts a set of matched node pairs with desired properties including one-to-one matching and mutual alignment.*

Proof. The conclusion is easily obtained according to the property of the maximum weight matching algorithms. \square

Algorithm 6: The Combine Module**Input:** Embedding & OT-based outputs, $\mathbf{T}_{WL}, \mathbf{T}_{GW}$ **Output:** The combined prediction \mathcal{M}

```

1 Construct bipartite graph  $\mathcal{G}_b$  with  $\mathcal{V}_b \leftarrow \mathcal{V}_s \cup \mathcal{V}_t$ ;
2 Construct  $\mathcal{E}_b$  by row-wise top- $r$  prediction of  $\mathbf{T}_{GW}$ ;
3  $\mathcal{E}_b.weight \leftarrow g_{EL}(\mathbf{T}_{WL}, \mathbf{T}_{GW})$ ;
4 Compute the maximum weight matching  $\mathcal{M}$  for  $\mathcal{G}_b$ ;
5 return  $\mathcal{M}$ ;

```

D. Algorithm Analysis and Optimization

1) Complexity Analysis: We discuss the complexity of CombAlign by analyzing each module in brief. The WL module takes $O(K(md + nd^2) + n^2 d)$ time, where the first term follows classical message-passing GNNs and the second term corresponds to the multiplication of two $n \times d$ -sized embedding matrices. The NUM module only incurs $O(n^2)$ time for the matrix-vector multiplication. The GRAFT module

TABLE II
COMPARISON OF MODEL COMPLEXITY WITH STATE OF THE ART.

Method	Time Complexity
GTCAAlign [16] (Emb.)	$O(IK(md + n^2d))$
SLOTAAlign [3] (OT)	$O(I(K(md + nd^2) + n^2d + I_{ot}n^3))$
CombAlign	$O(I(K(md + nd^2) + n^2d + I_{ot}n^3))$
CombAlign (Optimized)	$O(I(K(md + nd^2) + n^2(d + I_{ot}\log n)))$

has the same asymptotic complexity with SLOTAAlign [3] since the additional feature transformation only needs $O(Kd^2)$ time. To be more specific, for both the GRAFT module and SLOTAAlign, the cost computation of GW learning is $O(n^3)$ per round according to [17], with an inner-loop of I_{ot} rounds for the Proximal Point Method. For the Combine module, the bipartite graph construction step takes linear time, and the complexity is dominated by maximum weight matching. Although classical algorithms [30], [46], [45] typically need $O(n^3)$ time, note that our bipartite graph only contains $O(rn_1)$ edges, which corresponds to the *sparse* linear assignment problem with $O(n^2r)$ complexity [47]. This process can be further improved with faster matching algorithms [48], [49]. In sum, the asymptotic complexity is $O(I(K(md + nd^2) + n^2d + I_{ot}n^3))$, which is in the same order as other optimal transport-based alignment methods [17], [19], [18], [3]. In comparison, we also demonstrate the time complexity of two representative methods in Table II. Note that both embedding and OT-based methods need to iteratively update the alignment probabilities, thus we use I to represent the number of iterations.

2) *Optimizations*: According to our analysis, the asymptotic complexity of CombAlign (and other OT-based approaches) can be simplified to $O(n^3)$ since n dominates other inputs (i.e., I , K , and d). Unfortunately, a time complexity gap is observed between embedding-based solutions [15], [14], [16] and CombAlign, while the former only takes roughly $O(n^2)$ time. The complexity bottleneck of OT arises from the GWD cost computation (i.e., \mathbf{C}_{gwd}). According to [17], it can be reformalized as $\mathbf{C}_{gwd} = \mathbf{C}_s^2 \mu \mathbf{1}_{n_2}^T + \mathbf{1}_{n_1} \nu^T \mathbf{C}_t^2 - 2\mathbf{C}_s \mathbf{T} \mathbf{C}_t^T$, reducing the computational complexity from $O(n^4)$ to $O(n^3)$. (Note that the square operation is element-wise.) Since only the third term has a complexity of $O(n^3)$, we simplify the intra-graph cost design by only utilizing the adjacency matrix, which leads to a $\mathbf{A}_s \mathbf{T} \mathbf{A}_t^T$ term. For real-world graphs, the adjacency matrix is sparse, namely, the number of edges m is bounded by $O(n \log n)$ [50], and it holds that $m/n \ll d$ in practice (Cf. Section IV). To this end, multiplying two sparse matrices with a dense one can be fulfilled in $O(nm) = O(n \log n)$ time. We also employ powerful embedding learning models (e.g., [51]) in the GRAFT module to alleviate the degradation of model expressiveness. As shown in Table II, our optimized model successfully closes the complexity gap between two categories of learning-based approaches.

IV. EXPERIMENTS

We conduct a comprehensive experimental evaluation to answer the following key research questions:

- Q1. Does CombAlign outperform state of the art?
- Q2. How effective is each component of CombAlign?

TABLE III
DATASETS AND THEIR STATISTICS.

Dataset	n_1, n_2	m_1, m_2	Features	Anchors
Douban [24]	1, 118 3, 906	3, 022 16, 328	538	1, 118
ACM-DBLP [52]	9, 872 9, 916	39, 561 44, 808	17	6, 325
Allmovie-Imdb [14]	6, 011 5, 713	124, 709 119, 073	14	5, 174
Cora [53]	2, 708 2, 708	5, 028 5, 028	1, 433	2, 708
Citeseer [53]	3, 327 3, 327	4, 732 4, 732	3, 703	3, 327
PPI [54]	1, 767 1, 767	16, 159 16, 159	50	1, 767
CS [55]	18, 333 18, 333	114, 652 147, 410	6, 805	18, 333
Physics [55]	34, 493 34, 493	347, 147 446, 332	8, 415	34, 493

- Q3. Is CombAlign capable of holding matching properties such as one-to-one matching and mutual alignment?
- Q4. How efficient and scalable is CombAlign?

A. Experimental Settings

Datasets. Our experimental evaluation uses six well-adopted datasets for unsupervised graph alignment [3], [18], [16], [17], [15], including three real-world datasets Douban Online-Offline [24], ACM-DBLP [52], Allmovie-Imdb [14], as well as three synthetic ones, i.e., Cora [53], Citeseer [53], and PPI [54]. Moreover, we include two larger datasets for scalability analysis. The statistics of the datasets are listed in Table III. It is noteworthy that all ground truths provided in Table III are one-to-one node correspondences.

Baselines. We compare CombAlign with traditional solutions and representative embedding and OT-based models.

- *Traditional approaches.* We include KNN and use parameter-free GNNs to obtain node embeddings, based on which the top- k similar node pairs across graphs are matched. We also adopt the modified version of the Jonker-Volgenant algorithm [45] (MJV) for the linear assignment problem, which returns one-to-one alignment.
- *Embedding-based models.* We consider WAlign [15], which relies on GNNs with a Wasserstein distance discriminator to find node correspondences and two state of the arts with graph augmentation techniques [14], [16].
- *OT-based models.* This includes GWL [17], SLOTAAlign [3], and UHOT-GM [18], all based on the GW learning process but with increasingly sophisticated design of intra-graph cost, from hand-designed functions and learnable node embeddings [17] to node feature propagation and multiple cost terms [3], [18].

We omit other learning-based methods (e.g., [19], [44]) as they have been surpassed by the above baselines according to existing literature [15], [16], [17], [3].

TABLE IV
COMPARISON OF MODEL PERFORMANCE ON SIX DATASETS.

Datasets	Metrics	KNN	GAlign	WAlign	GTCAAlign	GWL	SLOTAlign	UHOT-GM	CombAlign w/o C
Douban	Hits@1	27.82	45.26	39.45	<u>61.79</u>	3.29	51.43	60.23	68.52
	Hits@5	45.53	67.71	62.35	<u>76.83</u>	8.32	73.43	71.36	87.84
	Hits@10	52.68	78.00	71.47	<u>82.29</u>	9.93	77.73	76.91	91.41
	MAP	36.08	56.32	46.22	<u>69.77</u>	5.79	61.29	67.35	77.08
ACM-DBLP	Hits@1	36.35	<u>70.20</u>	63.43	60.92	56.36	66.04	69.89	72.18
	Hits@5	66.83	<u>87.23</u>	83.18	75.60	77.09	85.84	87.12	88.98
	Hits@10	76.22	<u>91.36</u>	86.58	79.97	82.18	87.76	90.65	92.63
	MAP	50.11	<u>77.49</u>	70.76	67.67	64.82	73.76	77.18	79.55
Allmovie-Imdb	Hits@1	32.39	82.14	52.61	84.73	87.82	90.60	<u>91.73</u>	96.25
	Hits@5	51.57	86.35	70.91	89.89	92.31	92.75	<u>94.36</u>	97.66
	Hits@10	58.79	90.03	76.52	91.32	92.83	93.14	<u>94.96</u>	97.89
	MAP	41.50	84.96	61.17	87.12	89.64	91.61	<u>92.74</u>	97.31
Cora	Hits@	95.01	99.45	98.45	99.35	86.19	<u>99.48</u>	<u>99.48</u>	99.56
	Hits@5	100	100	100	100	93.61	100	100	100
	Hits@10	100	100	100	100	94.57	100	100	100
	MAP	98.66	99.69	99.18	99.69	89.71	99.71	<u>99.72</u>	99.75
Citeseer	Hits@1	89.72	<u>99.73</u>	97.81	99.68	57.05	99.25	99.47	99.82
	Hits@5	100	100	100	100	65.04	100	100	100
	Hits@10	100	100	100	100	65.95	100	100	100
	MAP	94.91	99.84	98.88	<u>99.89</u>	61.31	99.62	99.69	99.91
PPI	Hits@1	84.96	89.20	88.51	89.25	86.76	89.30	89.33	89.70
	Hits@5	89.10	90.64	<u>93.10</u>	92.81	88.06	92.53	92.97	93.15
	Hits@10	92.17	94.16	<u>94.17</u>	94.07	88.62	93.49	93.52	94.85
	MAP	87.65	90.72	89.02	<u>90.80</u>	87.74	90.76	90.81	91.12

Evaluation Metrics. Following previous studies [3], [18], [16], [15], we adopt Hits@ k with $k = \{1, 5, 10\}$ and Mean Average Precision (MAP) to evaluate the model performance. Given the ground truth \mathcal{M}^* , for each $(u, v) \in \mathcal{M}^*$ with $u \in \mathcal{G}_s$ and $v \in \mathcal{G}_t$, we check if v belongs to the top- k predictions ordered by alignment probability, denoted as $S_k(u)$. Then, Hits@ k is computed as follows:

$$\text{Hits@}k = \frac{\sum_{(u,v) \in \mathcal{M}^*} \mathbb{1}[v \in S_k(u)]}{|\mathcal{M}^*|}, \quad (17)$$

where $\mathbb{1}[\cdot]$ is the indicator function which equals 1 if the condition holds. MAP is employed to evaluate the accuracy of the predicted node rankings:

$$\text{MAP} = \frac{\sum_{(u_i, v_k) \in \mathcal{M}^*} \frac{1}{\text{Rank}(u_i, v_k)}}{|\mathcal{M}^*|}, \quad (18)$$

where $\text{Rank}(u_i, v_k)$ denotes the ranking of v_k according to $\mathbf{T}(i, \cdot)$ by descending order.

Implementation Details. For all baselines, we obtain the source code from the authors. Our model is implemented based on PyTorch 1.12.1 and PyTorch Geometric. Specifically, for CombAlign, we set the feature dimension d as 32 and the graph convolution layers K as 3. The learning rates τ_β and τ_W for updating β and W are set to 1 and 0.01, respectively. All experiments are conducted on a high-performance computing server with a GeForce RTX 4090 GPU equipped with 24 GB of memory. The source code will be made publicly available upon the acceptance of the paper.

B. Experimental Results

1) *Model Performance:* CombAlign **w/o the Combine module** (CombAlign w/o C). We first evaluate the predic-

TABLE V
COMPARISON OF HITS@1 WITH ONE-TO-ONE MATCHING CONSTRAINT.

Datasets	Douban	ACM-DBLP	Allmovie-Imdb
KNN	23.88	31.11	28.79
MJV	31.03	56.89	35.14
GAlign	20.84	66.18	80.28
WAlign	15.56	60.33	51.29
GTCAAlign	57.15	56.96	83.91
GWL	3.22	52.09	87.22
SLOTAlign	49.19	64.32	90.31
UHOT-GM	<u>58.31</u>	<u>67.78</u>	<u>91.26</u>
CombAlign	70.75	74.19	96.57

TABLE VI
THE PERFORMANCE (HITS@1) OF GRAFT WITH DIFFERENT GNNs.

Hits@1	Douban	ACM-DBLP	Allmovie-Imdb
w/ LGCN	57.07	68.87	93.39
w/ GCN	61.45	69.68	94.57
w/ GIN	63.15	71.64	95.61
w/ SGFormer	65.38	72.73	96.02

tion accuracy following previous learning-based settings [3], [16], specifically, the output is formulated as the alignment probability matrix. As shown in Table IV, we use the bold font to highlight the best result and underline the second-best values². As for the baselines, note that GAlign achieves the best performance on ACM-DBLP while UHOT-GM has the highest accuracy on Allmovie-Imdb. For the Douban dataset, GTCAAlign and UHOT-GM are the two best baselines. It can be concluded that neither OT-based methods nor embed-

²The reported figures are the average of five independent rounds, and we omit the standard errors following most existing work because the prediction accuracy is highly concentrated for this problem.

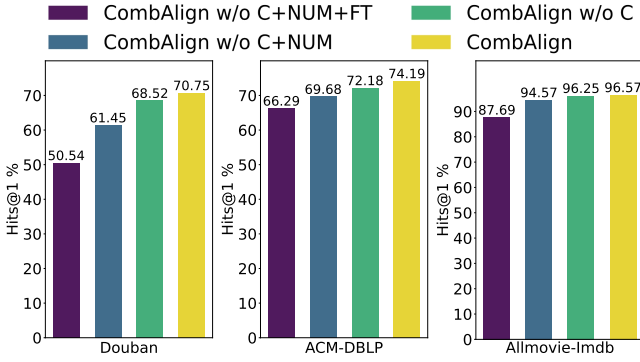


Fig. 5. Ablation study on three real-world datasets.

ding solutions can consistently outperform the other. For the embedding-based algorithms, we note that there does not exist a clear winner between GAlign and GTCAAlign on the real-world datasets, demonstrating the limitation of the embedding-only heuristics in the unsupervised setting. Nonetheless, both of them outperform WAlign, while the training process of the latter encounters significant oscillations, partially due to the challenges in training GANs [56], [57]. For the OT-based methods, it is clear that more sophisticated design of intra-graph costs by considering multiple terms (i.e., SLOAlign) and cross-modal comparison (i.e., UHOT-GM) results in better practical accuracy.

For the CombAlign w/o C algorithm, in our experiments, we adopt GCN [40] as the default GNN modules in GRAFT and WL. It consistently demonstrates superior performance across all evaluation metrics on three real-world datasets, validating the effectiveness of our model. Notably, on the Douban and Allmovie-Imdb datasets, it achieves significant improvements in Hits@1, with relative gains of 10.89% and 4.93%, respectively. For the synthetic datasets, CombAlign w/o C also has the highest performance.

CombAlign (w/ the Combine module). As presented in Table V, we evaluate CombAlign against the baselines by forcing the one-to-one matching constraint. Among the evaluated methods, only MJV and CombAlign inherently ensure one-to-one matching, as they directly output matched node pairs. For other methods generating the alignment probabilities, we eliminate all one-to-many predictions by retaining only the node pair with the highest probability. (Also note that mutual alignment is non-trivial to obtain for these methods.) It is observed that these methods inevitably suffer from performance degradation in this setting (Cf. Table IV), and the phenomenon is significant on Douban and ACM-DBLP.

In comparison, CombAlign consistently outperforms all other methods. Notably, the substantial improvement of CombAlign over MJV underscores the critical role of weight design and demonstrates the effectiveness of the proposed ensemble learning strategy. Compared to CombAlign w/o C, CombAlign not only ensures one-to-one matching (and mutual alignment) but also significantly enhances performance.

2) *Ablation Study:* To test the effectiveness of each module, we progressively remove Combine, NUM, and feature transformation in GRAFT. The resulting model variants are

as follows. For CombAlign w/o C, we make predictions by T_{GW} because it generally achieves higher accuracy by combining the prior knowledge from WL. CombAlign w/o C+NUM further eliminates the NUM and WL modules, therefore, the uniform marginal is adopted. The CombAlign w/o C+NUM+FT variant removes feature transformation as well as feature propagation, resulting in a model theoretically weaker than SLOAlign.

We show the results of the ablation study in Figure 5. It is clear that all proposed modules have non-negligible contributions to model accuracy. More specifically, the Combine module boosts the accuracy on Douban (resp. ACM-DBLP) by more than two points. The non-uniform marginal and feature transformation significantly increase the model performance. For CombAlign w/o C+NUM+FT, the accuracy is close to SLOAlign, which coincides with the fact that the two models have minor differences.

3) *Further Evaluation of Different Modules:* We conduct a more extensive investigation of the proposed modules.

GRAFT with different GNNs. According to the theoretical results of Corollary III.3, more expressive GNNs should lead to better model accuracy. As shown in Table VI, we employ the CombAlign w/o C+NUM variant to test the lightweight GCN, GCN, and GIN (Cf. Section III-B1). We also include an efficient Graph Transformer [51] with even more representation power. The result nicely matches our theoretical conclusion.

Note that by default the GRAFT module uses GCN (e.g., for Table IV). We also point out that the GIN variant in Table VI has already outperformed all baselines shown in Table IV. We believe there is still room for further improvements with more powerful GNNs (and Graph Transformers).

Baselines with the Combine module. Next, we validate our Combine module for improving existing OT-based solutions. We substitute the GRAFT module with GWL, SLOAlign and UHOT-GM, and report the final prediction with Combine. As shown in Table VII, all methods achieve a significant enhancement of Hits@1, further validating the effectiveness of our Combine module.

One-to-one matching property of CombAlign. In Table VIII, we show the ratio of the remaining set compared to the ground truth set after eliminating one-to-many predictions for all model variants of CombAlign. This step is similar to that of Figure 4 (see Section III-C), in which we demonstrate the ratio of one-to-many predictions for our baselines. Consistent with our analysis, CombAlign manages to return a set of node pairs with one-to-one matching. Other variants of CombAlign also ensures higher similarity between matched pairs compared to the baselines.

4) *Convergence Analysis:* We simultaneously visualize the prediction accuracy and the model loss (i.e., Equation 1) on three real-world datasets at different epochs, as shown in Figure 6. With the increase of epochs, the loss gradually decreases to almost approaching zero, meanwhile, the Hits@1 value gradually converges.

5) *Model Efficiency and Scalability:* For model efficiency, we compare the running time of all methods in Figure 7 on three well-adopted datasets. It can be observed that KNN and

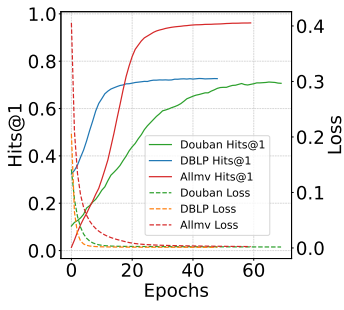
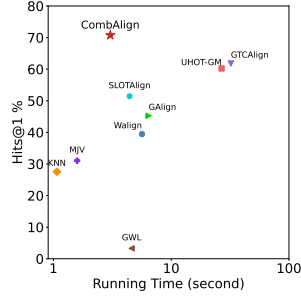
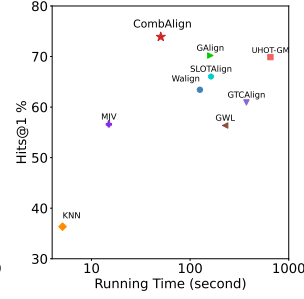


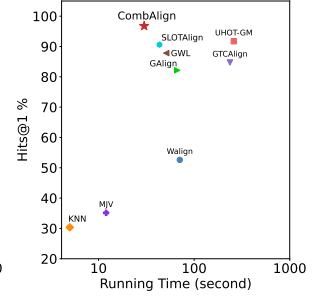
Fig. 6. Convergence Analysis.



(a) Douban



(b) ACM-DBLP



(c) Allmovie-Imdb

Fig. 7. Running time vs. Hits@1 of different methods.

TABLE VII
IMPROVING OTHER OT-BASED MODELS W/ COMBINE (HITS@1).

Methods	Douban	ACM-DBLP	Allmovie-Imdb
GWL	3.29	56.36	87.82
GWL+C	5.81	63.46	90.07
SLOAlign	51.43	66.04	90.60
SLOAlign+C	60.01	69.20	91.03
UHOT-GM	60.23	69.89	91.73
UHOT-GM+C	63.17	71.32	92.45

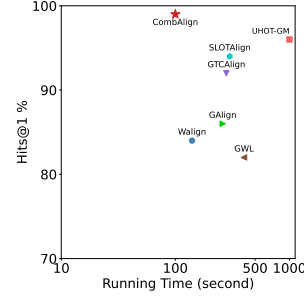
TABLE VIII
THE RATIO OF THE REMAINING SET OVER GROUND TRUTH AFTER
ELIMINATING ONE-TO-MANY PREDICTIONS.

CombAlign	Douban	ACM-DBLP	Allmovie-Imdb
- w/ C	100%	100%	100%
- w/o C	94.36%	88.36%	98.54%
- w/o C+NUM	94.18%	86.50%	97.60%
- w/o C+NUM+FT	91.32%	83.27%	96.25%

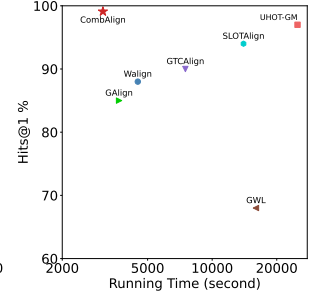
MJV achieve the highest efficiency but suffer from poor performance. Our proposed CombAlign has the best efficiency among all learning-based methods while maintaining the highest accuracy. This can be attributed to the strong expressive power of our model, which facilitates faster convergence. In terms of CombAlign, the GW learning process takes the majority of the time, while the additional costs of WL and Combine modules are negligible.

We also incorporate two larger datasets (i.e., CS and Physics) for scalability analysis compared to the SOTA baselines [14], [3], [18] (Figure 8). (We omit KNN and MJV for better readability.) For the CS dataset, it can reside in a GPU of 24GB memory, while for Physics, the $O(n^2)$ space cost for the alignment probability matrix exceeds the GPU memory size for both embedding and OT-based methods, and we conduct experiments with the CPU. On both datasets, the optimized CombAlign achieves the best results for efficiency and accuracy.

6) *Sensitivity Analysis*: To examine the impact of different hyper-parameters, on three real datasets including Douban, ACM-DBLP and Allmovie-Imdb, we analyze the performance of CombAlign with different feature dims $d \in \{16, 32, 64, 128, 256\}$ and the number of graph convolution layers $K \in \{2, 3, 4, 5\}$, as illustrated in Figure 9. In general, the model performance is stable w.r.t. d . Meanwhile, the accuracy declines when K exceeds 3, consistent with the



(a) CS



(b) Physics

Fig. 8. Scalability analysis.

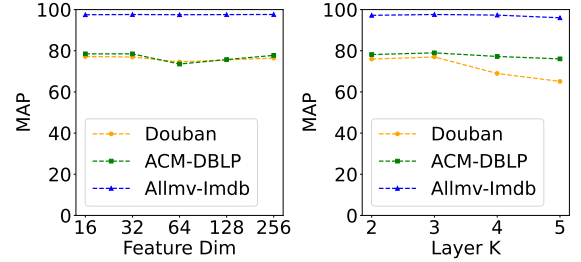


Fig. 9. Impact of hyper-parameters on CombAlign.

oversmoothing phenomenon of GNNs.

V. RELATED WORK

Unsupervised Graph Alignment. Classic graph alignment methods, such as EigenAlign [8], formulate the problem as a Quadratic Assignment Problem [8], [9], [10] which consider both matches and mismatches and solves it by spectral decomposition of matrices. Meanwhile, LREA [58] addresses the problem by solving a maximum weight bipartite matching problem on a low-rank approximation of a node-similarity matrix, and GRASP [44] treats the problem as a special case of finding a mapping between functions on graphs with the linear assignment algorithm.

In recent years, the research focus has shifted towards learning-based methods, which predict an alignment matrix indicating the matching probability for every node pair across two graphs. Existing unsupervised solutions can be roughly divided into two categories. The first category, referred to as “embed-then-cross-compare” [14], [15], [16], [59], [60], [61],

tackles the problem by first generating node representation for both graphs, e.g., using GNNs. Then, the alignment probability of two nodes is computed by specific similarity measures based on their embeddings, for example, the dot product [16], [14]. In particular, GAlign [14] incorporates the idea of data augmentation into the learning objective to obtain high-quality node embeddings. GTCAlign [16] further simplifies GAlign by using a GNN with randomized parameters for node embedding computation. Another recent work [15] conducts unsupervised graph alignment via the idea of generative adversarial network (GAN).

Instead of designing sophisticated alignment rules based on node embeddings, the second category [17], [3], [23], [18], [62], [63] of work is known as *optimal transport (OT)*-based approaches. They share the well-defined objective of minimizing Gromov-Wasserstein discrepancy, which predicts the alignment probabilities given the transport cost between node pairs. These methods mainly differ in the specific form of the *learnable* transport cost. GWL [17] is the first work following this paradigm with predefined cost and incorporates Wasserstein discrepancy and reconstruction loss for regularization. As the state-of-the-art approach, SLOAlign [3] extends GWL by multi-view structure modeling, which includes the linear combination of adjacency information, node features, and feature propagation. The most recent work, UHOT-GM [18], generalizes this idea with the notion of multiple and cross-modal alignment.

Semi-Supervised Graph Alignment. Unlike unsupervised graph alignment, with a set of anchor node pairs as input, the main idea of semi-supervised methods is to fully utilize the anchor information. A line of consistency-based algorithms [24], [5], [64], [65] is proposed to first define the neighborhood topology and attribute consistency followed by devising a procedure to propagate the anchor information across graphs, e.g., via Random Walk with Restart (RWR). Follow-up works resort to embedding-based approaches [66], [25], [67], [68], [69], [26], [27], [28], i.e., by learning node embeddings to make the anchor pairs close while preserving the graph structure in the latent space. A very recent work [23] incorporates the idea of optimal transport to better model the alignment consistency. Along with the RWR-based transport cost design, state-of-the-art performance is achieved.

Knowledge Graph Entity Alignment. A similar problem has been extensively studied [70], [71], [72], which aligns the entities across knowledge graphs [73]. For this problem setting, both topological structures and the semantics of features are important. Building upon optimal transport, FGWEA [74] proposes a fused Gromov-Wasserstein framework for unsupervised knowledge graph entity alignment, which effectively integrates structural and semantic information to achieve robust performance. Recent advance [75] has explored leveraging large language models (LLMs) to enhance knowledge graph entity alignment with richer textual information from diverse corpora. A more comprehensive review can be referred to [76], [77].

VI. CONCLUSION AND FUTURE WORK

In this paper, we formally investigate the model expressiveness for unsupervised graph alignment from two theoretical perspectives. We characterize the model's discriminative power as correctly distinguishing matched and unmatched node pairs across graphs and study the model's capability of guaranteeing important matching properties including one-to-one node matching and mutual alignment. Then, we propose a hybrid model named CombAlign to combine the advantages of both optimal transport and embedding-based solutions, which leads to provably more discriminative power. Our method is further empowered by ensembling both OT and embedding-based predictions with a traditional algorithm-inspired strategy, i.e., maximum weight matching, to guarantee the matching properties. Extensive experiments demonstrate significant improvements in alignment accuracy and the effectiveness of the proposed modules. Moreover, our theoretical analysis of expressive power is confirmed.

Although our CombAlign algorithm demonstrates remarkable improvements in terms of model performance and efficiency, the scalability issue with respect to the running time as well as the space cost remains a challenge for both categories of learning-based approaches. We leave this as the main focus of our future research.

ACKNOWLEDGMENTS

The authors would like to thank Prof. Lei Chen, Prof. Xiaofang Zhou, and Prof. Zhi Jin for fruitful discussions, and Haoran Cheng, Prof. Dixin Luo, and Prof. Hongteng Xu for their help in providing the baseline codes. This work is supported by NSFC under grants 62202037, 62372031, and 62372034.

REFERENCES

- [1] J. Zhang and S. Y. Philip, "Multiple anonymized social networks alignment," in *2015 IEEE International Conference on Data Mining*. IEEE, 2015, pp. 599–608.
- [2] C. Li, S. Wang, H. Wang, Y. Liang, P. S. Yu, Z. Li, and W. Wang, "Partially shared adversarial learning for semi-supervised multi-platform user identity linkage," in *Proceedings of the 28th ACM international conference on information and knowledge management*, 2019, pp. 249–258.
- [3] J. Tang, W. Zhang, J. Li, K. Zhao, F. Tsung, and J. Li, "Robust attributed graph alignment via joint structure learning and optimal transport," in *2023 IEEE 39th International Conference on Data Engineering (ICDE)*. IEEE, 2023, pp. 1638–1651.
- [4] J. Tang, J. Zhang, L. Yao, J. Li, L. Zhang, and Z. Su, "Arnetminer: extraction and mining of academic social networks," in *Proceedings of the 14th ACM SIGKDD international conference on Knowledge discovery and data mining*, 2008, pp. 990–998.
- [5] S. Zhang, H. Tong, L. Jin, Y. Xia, and Y. Guo, "Balancing consistency and disparity in network alignment," in *Proceedings of the 27th ACM SIGKDD conference on knowledge discovery & data mining*, 2021, pp. 2212–2222.
- [6] F. Bernard, J. Thunberg, P. Gemmar, F. Hertel, A. Husch, and J. Goncalves, "A solution for multi-alignment by transformation synchronisation," in *Proceedings of the IEEE conference on computer vision and pattern recognition*, 2015, pp. 2161–2169.
- [7] S. Haller, L. Feineis, L. Hutschenreiter, F. Bernard, C. Rother, D. Kainmüller, P. Swoboda, and B. Savchynskyy, "A comparative study of graph matching algorithms in computer vision," in *European Conference on Computer Vision*. Springer, 2022, pp. 636–653.

- [8] S. Feizi, G. Quon, M. Recamonde-Mendoza, M. Medard, M. Kellis, and A. Jadbabaie, "Spectral alignment of graphs," *IEEE Transactions on Network Science and Engineering*, vol. 7, no. 3, pp. 1182–1197, 2019.
- [9] P. A. Karakasis, A. Konar, and N. D. Sidiropoulos, "Joint graph embedding and alignment with spectral pivot," in *Proceedings of the 27th ACM SIGKDD Conference on Knowledge Discovery & Data Mining*, 2021, pp. 851–859.
- [10] J. Peng, H. Mittelman, and X. Li, "A new relaxation framework for quadratic assignment problems based on matrix splitting," *Mathematical Programming Computation*, vol. 2, pp. 59–77, 2010.
- [11] M. Bayati, M. Gerritsen, D. F. Gleich, A. Saberi, and Y. Wang, "Algorithms for large, sparse network alignment problems," in *ICDM 2009, The Ninth IEEE International Conference on Data Mining, Miami, Florida, USA, 6-9 December 2009*. IEEE Computer Society, 2009, pp. 705–710.
- [12] G. W. Klau, "A new graph-based method for pairwise global network alignment," *BMC Bioinform.*, vol. 10, no. S-1, 2009. [Online]. Available: <https://doi.org/10.1186/1471-2105-10-S1-S59>
- [13] R. Singh, J. Xu, and B. Berger, "Pairwise global alignment of protein interaction networks by matching neighborhood topology," in *Research in Computational Molecular Biology, 11th Annual International Conference, RECOMB 2007, Oakland, CA, USA, April 21-25, 2007, Proceedings*, ser. Lecture Notes in Computer Science, vol. 4453. Springer, 2007, pp. 16–31.
- [14] H. T. Trung, T. Van Vinh, N. T. Tam, H. Yin, M. Weidlich, and N. Q. V. Hung, "Adaptive network alignment with unsupervised and multi-order convolutional networks," in *2020 IEEE 36th International Conference on Data Engineering (ICDE)*. IEEE, 2020, pp. 85–96.
- [15] J. Gao, X. Huang, and J. Li, "Unsupervised graph alignment with wasserstein distance discriminator," in *Proceedings of the 27th ACM SIGKDD Conference on Knowledge Discovery & Data Mining*, 2021, pp. 426–435.
- [16] C. Wang, P. Jiang, X. Zhang, P. Wang, T. Qin, and X. Guan, "Gtalign: Global topology consistency-based graph alignment," *IEEE Transactions on Knowledge and Data Engineering*, 2023.
- [17] H. Xu, D. Luo, H. Zha, and L. C. Duke, "Gromov-wasserstein learning for graph matching and node embedding," in *International conference on machine learning*. PMLR, 2019, pp. 6932–6941.
- [18] H. Cheng, D. Luo, and H. Xu, "Dhot-gm: Robust graph matching using a differentiable hierarchical optimal transport framework," *arXiv preprint arXiv:2310.12081*, 2023.
- [19] V. Titouan, N. Courty, R. Tavenard, and R. Flamary, "Optimal transport for structured data with application on graphs," in *International Conference on Machine Learning*. PMLR, 2019, pp. 6275–6284.
- [20] C. Villani *et al.*, *Optimal transport: old and new*, 2009, vol. 338.
- [21] G. Peyré, M. Cuturi, and J. Solomon, "Gromov-wasserstein averaging of kernel and distance matrices," in *International conference on machine learning*. PMLR, 2016, pp. 2664–2672.
- [22] M. Kolář, J. Meier, V. Mustonen, M. Lässig, and J. Berg, "Graphalignment: Bayesian pairwise alignment of biological networks," *BMC systems biology*, vol. 6, pp. 1–12, 2012.
- [23] Z. Zeng, S. Zhang, Y. Xia, and H. Tong, "Parrot: Position-aware regularized optimal transport for network alignment," in *Proceedings of the ACM Web Conference 2023*, 2023, pp. 372–382.
- [24] S. Zhang and H. Tong, "Final: Fast attributed network alignment," in *Proceedings of the 22nd ACM SIGKDD international conference on knowledge discovery and data mining*, 2016, pp. 1345–1354.
- [25] Y. Yan, S. Zhang, and H. Tong, "Bright: A bridging algorithm for network alignment," in *Proceedings of the web conference 2021*, 2021, pp. 3907–3917.
- [26] L. Liu, P. Chen, X. Li, W. K. Cheung, Y. Zhang, Q. Liu, and G. Wang, "Wl-align: Weisfeiler-lehman relabeling for aligning users across networks via regularized representation learning," *IEEE Transactions on Knowledge and Data Engineering*, vol. 36, no. 1, pp. 445–458, 2023.
- [27] N. Ning, B. Wu, H. Ren, and Q. Li, "Graph alignment neural network model with graph to sequence learning," *IEEE Transactions on Knowledge and Data Engineering*, 2023.
- [28] T. T. Huynh, C. T. Duong, T. T. Nguyen, V. T. Van, A. Sattar, H. Yin, and Q. V. H. Nguyen, "Network alignment with holistic embeddings," *IEEE Transactions on Knowledge and Data Engineering*, vol. 35, no. 2, pp. 1881–1894, 2021.
- [29] N. Shervashidze, P. Schweitzer, E. J. Van Leeuwen, K. Mehlhorn, and K. M. Borgwardt, "Weisfeiler-lehman graph kernels," *Journal of Machine Learning Research*, vol. 12, no. 9, 2011.
- [30] J. Edmonds and R. M. Karp, "Theoretical improvements in algorithmic efficiency for network flow problems," *Journal of the ACM (JACM)*, vol. 19, no. 2, pp. 248–264, 1972.
- [31] R. Jonker and T. Volgenant, "A shortest augmenting path algorithm for dense and sparse linear assignment problems," in *DGOR/NSOR: Papers of the 16th Annual Meeting of DGOR in Cooperation with NSOR/Vorträge der 16. Jahrestagung der DGOR zusammen mit der NSOR*. Springer, 1988, pp. 622–622.
- [32] Z.-H. Zhou, *Ensemble methods: foundations and algorithms*. CRC press, 2012.
- [33] T. G. Dietterich, "Ensemble methods in machine learning," in *International workshop on multiple classifier systems*. Springer, 2000, pp. 1–15.
- [34] M. Cuturi, "Sinkhorn distances: Lightspeed computation of optimal transport," *Advances in neural information processing systems*, vol. 26, 2013.
- [35] R. Sinkhorn and P. Knopp, "Concerning nonnegative matrices and doubly stochastic matrices," *Pacific Journal of Mathematics*, vol. 21, no. 2, pp. 343–348, 1967.
- [36] Y. Xie, X. Wang, R. Wang, and H. Zha, "A fast proximal point method for computing exact wasserstein distance," in *Uncertainty in artificial intelligence*. PMLR, 2020, pp. 433–453.
- [37] G. Corso, H. Stark, S. Jegelka, T. Jaakkola, and R. Barzilay, "Graph neural networks," *Nature Reviews Methods Primers*, vol. 4, no. 1, p. 17, 2024.
- [38] G. Lv and L. Chen, "On data-aware global explainability of graph neural networks," *Proceedings of the VLDB Endowment*, vol. 16, no. 11, pp. 3447–3460, 2023.
- [39] C. T. Duong, T. D. Hoang, H. Yin, M. Weidlich, Q. V. H. Nguyen, and K. Aberer, "Efficient streaming subgraph isomorphism with graph neural networks," *Proceedings of the VLDB Endowment*, vol. 14, no. 5, pp. 730–742, 2021.
- [40] T. N. Kipf and M. Welling, "Semi-supervised classification with graph convolutional networks," *arXiv preprint arXiv:1609.02907*, 2016.
- [41] P. Veličković, G. Cucurull, A. Casanova, A. Romero, P. Lio, and Y. Bengio, "Graph attention networks," *arXiv preprint arXiv:1710.10903*, 2017.
- [42] K. Xu, W. Hu, J. Leskovec, and S. Jegelka, "How powerful are graph neural networks?" *arXiv preprint arXiv:1810.00826*, 2018.
- [43] F. Wu, A. Souza, T. Zhang, C. Fifty, T. Yu, and K. Weinberger, "Simplifying graph convolutional networks," in *International conference on machine learning*. PMLR, 2019, pp. 6861–6871.
- [44] J. Hermanns, K. Skitsas, A. Tsitsulin, M. Munkhoeva, A. Kyster, S. Nielsen, A. M. Bronstein, D. Mottin, and P. Karras, "Grasp: Scalable graph alignment by spectral corresponding functions," *ACM Transactions on Knowledge Discovery from Data*, vol. 17, no. 4, pp. 1–26, 2023.
- [45] D. F. Crouse, "On implementing 2d rectangular assignment algorithms," *IEEE Transactions on Aerospace and Electronic Systems*, vol. 52, no. 4, pp. 1679–1696, 2016.
- [46] J. Munkres, "Algorithms for the assignment and transportation problems," *Journal of the society for industrial and applied mathematics*, vol. 5, no. 1, pp. 32–38, 1957.
- [47] H. Cui, J. Zhang, C. Cui, and Q. Chen, "Solving large-scale assignment problems by kuhn-munkres algorithm," in *2nd international conference on advances in mechanical engineering and industrial informatics (AMEII 2016)*, 2016, pp. 822–827.
- [48] B. Schwartz, "A computational analysis of the auction algorithm," *European journal of operational research*, vol. 74, no. 1, pp. 161–169, 1994.
- [49] L. Buš and P. Tvrdík, "Towards auction algorithms for large dense assignment problems," *Computational Optimization and Applications*, vol. 43, pp. 411–436, 2009.
- [50] S. Wang, R. Yang, X. Xiao, Z. Wei, and Y. Yang, "Fora: simple and effective approximate single-source personalized pagerank," in *Proceedings of the 23rd ACM SIGKDD International Conference on Knowledge Discovery and Data Mining*, 2017, pp. 505–514.
- [51] Q. Wu, W. Zhao, C. Yang, H. Zhang, F. Nie, H. Jiang, Y. Bian, and J. Yan, "Sgformer: Simplifying and empowering transformers for large-graph representations," *Advances in Neural Information Processing Systems*, vol. 36, pp. 64 753–64 773, 2023.
- [52] S. Zhang and H. Tong, "Attributed network alignment: Problem definitions and fast solutions," *IEEE Transactions on Knowledge and Data Engineering*, vol. 31, no. 9, pp. 1680–1692, 2018.
- [53] P. Sen, G. Namata, M. Bilgic, L. Getoor, B. Galligher, and T. Eliassi-Rad, "Collective classification in network data," *AI magazine*, vol. 29, no. 3, pp. 93–93, 2008.

- [54] M. Zitnik and J. Leskovec, "Predicting multicellular function through multi-layer tissue networks," *Bioinformatics*, vol. 33, no. 14, pp. i190–i198, 2017.
- [55] O. Shchur, M. Mumme, A. Bojchevski, and S. Günnemann, "Pitfalls of graph neural network evaluation," *arXiv preprint arXiv:1811.05868*, 2018.
- [56] I. Gulrajani, F. Ahmed, M. Arjovsky, V. Dumoulin, and A. C. Courville, "Improved training of wasserstein gans," *Advances in neural information processing systems*, vol. 30, 2017.
- [57] M. Arjovsky, S. Chintala, and L. Bottou, "Wasserstein generative adversarial networks," in *Proceedings of the 34th International Conference on Machine Learning, ICML 2017, Sydney, NSW, Australia, 6-11 August 2017*, 2017.
- [58] H. Nassar, N. Veldt, S. Mohammadi, A. Grama, and D. F. Gleich, "Low rank spectral network alignment," in *Proceedings of the 2018 World Wide Web Conference*, 2018, pp. 619–628.
- [59] L. Liu, W. K. Cheung, X. Li, and L. Liao, "Aligning users across social networks using network embedding," in *Ijcai*, vol. 16, 2016, pp. 1774–80.
- [60] Q. Sun, X. Lin, Y. Zhang, W. Zhang, and C. Chen, "Towards higher-order topological consistency for unsupervised network alignment," in *2023 IEEE 39th International Conference on Data Engineering (ICDE)*. IEEE, 2023, pp. 177–190.
- [61] J. Peng, F. Xiong, S. Pan, L. Wang, and X. Xiong, "Robust network alignment with the combination of structure and attribute embeddings," in *2023 IEEE International Conference on Data Mining (ICDM)*. IEEE, 2023, pp. 498–507.
- [62] H. Petric Maretic, M. El Gheche, G. Chierchia, and P. Frossard, "Got: an optimal transport framework for graph comparison," *Advances in Neural Information Processing Systems*, vol. 32, 2019.
- [63] L. Chen, Z. Gan, Y. Cheng, L. Li, L. Carin, and J. Liu, "Graph optimal transport for cross-domain alignment," in *International Conference on Machine Learning*. PMLR, 2020, pp. 1542–1553.
- [64] R. Singh, J. Xu, and B. Berger, "Global alignment of multiple protein interaction networks with application to functional orthology detection," *Proceedings of the National Academy of Sciences*, vol. 105, no. 35, pp. 12 763–12 768, 2008.
- [65] D. Koutra, H. Tong, and D. Lubensky, "Big-align: Fast bipartite graph alignment," in *2013 IEEE 13th international conference on data mining*. IEEE, 2013, pp. 389–398.
- [66] S. Zhang, H. Tong, Y. Xia, L. Xiong, and J. Xu, "Nettrans: Neural cross-network transformation," in *Proceedings of the 26th ACM SIGKDD International Conference on Knowledge Discovery & Data Mining*, 2020, pp. 986–996.
- [67] M. Heimann, H. Shen, T. Safavi, and D. Koutra, "Regal: Representation learning-based graph alignment," in *Proceedings of the 27th ACM international conference on information and knowledge management*, 2018, pp. 117–126.
- [68] Q. Zhou, L. Li, X. Wu, N. Cao, L. Ying, and H. Tong, "Attent: Active attributed network alignment," in *Proceedings of the Web Conference 2021*, 2021, pp. 3896–3906.
- [69] H. Hong, X. Li, Y. Pan, and I. W. Tsang, "Domain-adversarial network alignment," *IEEE Transactions on Knowledge and Data Engineering*, vol. 34, no. 7, pp. 3211–3224, 2020.
- [70] Z. Wang, Q. Lv, X. Lan, and Y. Zhang, "Cross-lingual knowledge graph alignment via graph convolutional networks," in *Proceedings of the 2018 conference on empirical methods in natural language processing*, 2018, pp. 349–357.
- [71] Z. Sun, W. Hu, Q. Zhang, and Y. Qu, "Bootstrapping entity alignment with knowledge graph embedding," in *IJCAI*, vol. 18, no. 2018, 2018.
- [72] K. Zeng, C. Li, L. Hou, J. Li, and L. Feng, "A comprehensive survey of entity alignment for knowledge graphs," *AI Open*, vol. 2, pp. 1–13, 2021.
- [73] R. Zhang, B. D. Trisedya, M. Li, Y. Jiang, and J. Qi, "A benchmark and comprehensive survey on knowledge graph entity alignment via representation learning," *The VLDB Journal*, vol. 31, no. 5, pp. 1143–1168, 2022.
- [74] J. Tang, K. Zhao, and J. Li, "A fused gromov-wasserstein framework for unsupervised knowledge graph entity alignment," *arXiv preprint arXiv:2305.06574*, 2023.
- [75] X. Jiang, Y. Shen, Z. Shi, C. Xu, W. Li, Z. Li, J. Guo, H. Shen, and Y. Wang, "Unlocking the power of large language models for entity alignment," *arXiv preprint arXiv:2402.15048*, 2024.
- [76] W. Zeng, X. Zhao, Z. Tan, J. Tang, and X. Cheng, "Matching knowledge graphs in entity embedding spaces: An experimental study," *IEEE Transactions on Knowledge and Data Engineering*, vol. 35, no. 12, pp. 12 770–12 784, 2023.
- [77] B. Zhu, R. Wang, J. Wang, F. Shao, and K. Wang, "A survey: knowledge graph entity alignment research based on graph embedding," *Artificial Intelligence Review*, vol. 57, no. 9, p. 229, 2024.